Implication of DNA methylation changes at chromosome 1q21.1 in the brain pathology of Primary Progressive Multiple Sclerosis

Majid Pahlevan Kakhki[a], Chiara Starvaggi Cucuzza[a], Antonino Giordano[a,b,c], Tejaswi Venkata S. Badam[a,d], Pernilla Strid[a], Klementy Shchetynsky[a], Adil Harroud[e,f,g], Alexandra Gyllenberg[a], Yun Liu[h], Sanjaykumar Boddul[i], Tojo James[a], Melissa Sorosina[c], Massimo Filippi[b,j,k], Federica Esposito[b,c], Fredrik Wermeling[i], Mika Gustafsson[d], Patrizia Casaccia[l], Ingrid Kockum[a], Jan Hillert[a], Tomas Olsson[a], Lara Kular[a,1,2] and Maja Jagodic[a,1,2].

[a]Department of Clinical Neuroscience, Karolinska Institutet, Center for Molecular Medicine, Karolinska University Hospital, Stockholm, Sweden.

[b]Neurology and Neurorehabilitation Units, IRCCS San Raffaele Hospital, Milan, Italy

[c]Laboratory of Human Genetics of Neurological Disorders, Division of Neuroscience, San Raffaele Scientific Institute, Milan, Italy.

[d]Department of Bioinformatics, Institute for Physics chemistry and Biology (IFM), Linköping university, Linköping, Sweden.

[e]The Neuro (Montreal Neurological Institute-Hospital), Montréal, QC, Canada

[f]Department of Neurology and Neurosurgery, McGill University, Montréal, QC, Canada

[g]Department of Human Genetics, McGill University, Montréal, QC, Canada

[h]MOE Key Laboratory of Metabolism and Molecular Medicine, Department of Biochemistry and Molecular Biology, School of Basic Medical Sciences and Shanghai Xuhui Central Hospital, Fudan University, Shanghai, China.

[i]Department of Medicine, Solna, Karolinska Institutet, Center for Molecular Medicine, Karolinska University Hospital, Stockholm, Sweden.

[j]Neurophysiology Unit, IRCCS San Raffaele Hospital, Milan, Italy.

[k]Neuroimaging Research Unit, Division of Neuroscience, San Raffaele Scientific Institute, Milan, Italy.

[l]Department of Neurology, Icahn School of Medicine at Mount Sinai, New York, USA.

[1]Corresponding author: Maja Jagodic and Lara Kular, Department of Clinical Neuroscience, Karolinska Institutet, Center for Molecular Medicine, Karolinska University Hospital, Stockholm, Sweden. [2]Contributed equally

Email: maja.jagodic@ki.se and lara.kular@ki.se

Author Contributions: MJ conceptualized, designed, interpreted and supervised the study. MPK conducted the cloning, BS-pyrosequencing, in-vitro DNA methylation assays, dCas9-TET1 experiments and interpreted the data with the assistance of CSC. SB and FW assisted in lentiviral production and in-vitro experiments. YL performed genome-wide DNA methylation and meQTL analyses (cohort 1). AGy carried out locus-specific meQTL (cohort 2). AGi, PS, KS and AGy conducted genetic association analyses (cohort 3). AH performed phasing and imputation of genotypes. TVSB performed correlation network analysis and MG supervised network analysis. TJ aided in data acquisition. LK supervised the study, performed analyses, interpreted the data and wrote the manuscript with contribution from all co-authors. IK and FE provided genetic data. PC provided brain sequencing data. MS contributed to genotyping of the Italian cohort. MF, MS, FE, AGi, TO, JH and PC contributed to the collection of patient samples. All authors read and approved the final manuscript.

Competing Interest Statement: The authors declare that they have no competing interests.
Classification: Biological Sciences/Immunology and Inflammation.
Keywords: Multiple Sclerosis, progression, DNA methylation, CRISPR/dCas9, neurodegeneration.
This PDF file includes:

Main Text
Figure legends 1 to 5
Tables legend 1

Abstract

Multiple Sclerosis (MS) is a heterogeneous inflammatory and neurodegenerative disease of the central nervous system with an unpredictable course toward progressive disability. Understanding and treating progressive MS remains extremely challenging due to the limited knowledge of the underlying mechanisms. We examined the molecular changes associated with primary progressive MS (PPMS) using a cross-tissue (blood and post-mortem brain) and multilayered data (genetic, epigenetic, transcriptomic) from independent cohorts. We identified and replicated hypermethylation of an intergenic region within the chromosome 1q21.1 locus in the blood of PPMS patients compared to other MS patients and healthy individuals. We next revealed that methylation is under genetic control both in the blood and brain. Genetic analysis in the largest to date PPMS dataset yielded evidence of association of genetic variations in the 1q21.1 locus with PPMS risk. Several variants affected both 1q21.1 methylation and the expression of proximal genes (*CHD1L*, *PRKAB2*, *FMO5*) in the brain, suggesting a genetic-epigenetic-transcriptional interplay in PPMS pathogenesis. We addressed the causal link between methylation and expression using reporter systems and dCas9-TET1-induced CpG demethylation in the 1q21.1 region, which resulted in upregulation of *CHD1L* and *PRKAB2* genes in SH-SY5Y neuron-like cells. Independent exploration using unbiased correlation network analysis confirmed the putative implication of *CHD1L* and *PRKAB2* in brain processes in PPMS patients. Thus, several lines of evidence suggest that distinct molecular changes in 1q21.1 locus, known to be important for brain development and disorders, associate with genetic predisposition to high methylation in PPMS patients that regulates the expression of proximal genes.

Significance Statement

Multiple sclerosis (MS) is a long-lasting neurological disease affecting young individuals that occurs when the body's natural guard (immune system) attacks the brain cells. There are currently no efficient treatments for the progressive form of MS disease, probably because the mechanisms behind MS progression are still largely unknown. Thus, treatment of progressive MS remains the greatest challenge in managing patients. We aim to tackle this issue using the emerging field called "epigenetics" which has the potential to explain the impact of genetic and environmental risk factors in MS. In this project, by using unique clinical material and novel epigenetic tools, we identified new mechanisms involved in MS progression and putative candidates for targeted epigenetic therapy of progressive MS patients.

Main Text

Introduction

Multiple Sclerosis (MS) is an inflammatory disease of the central nervous system (CNS) affecting young adults and leading to unpredictable and progressive physical and cognitive impairments. The pathological hallmarks of MS are represented by focal plaques of primary demyelination and di use neurodegeneration in the grey and white matter of the brain and spinal cord (1). The most common form of disease, relapsing-remitting MS (RRMS), affects twice as many women as men and presents itself with neurological relapses followed by periods of partial or complete remission. In most cases, this inflammatory stage is followed by a secondary progressive phase of MS (SPMS) after several years. About 10-15% of patients, manifest a primary progressive form of MS disease (PPMS) with uninterrupted progression starting from disease onset, although relapses may occur (2). Beyond epidemiological differences, both progressive forms of MS share similar features that differ from RRMS stage, notably a later onset (40 years vs. 30 years in RRMS) and a prevalence of CNS-intrinsic inflammatory and degenerative pathological processes as opposed to the predominant role of peripheral immune influence in RRMS stage (3). However, while considerable progress has been achieved in deciphering the genetic variation predisposing for disease, the mechanisms underpinning disease progression and severity remain unresolved. Importantly, conventional immunomodulatory therapies are ineffective in progressive patients (4, 5), reinforcing the need to better clarify processes underlying MS courses.

Disease trajectory likely relies on a complex interplay between genetic and non-genetic factors (6). Epigenetic modifications such as DNA methylation, intersecting internal and external influences might provide novel opportunity to study the mechanisms underlying the different forms of MS disease. DNA methylation, which regulates gene expression without altering the genetic code, is the most studied epigenetic mark and its implications in MS pathogenesis have been reported in immune and nervous cells of MS patients (7-12). We have shown that the major risk variant *HLA-DRB1*15:01* may mediate risk for MS via changes in *HLA-DRB1* DNA methylation and subsequent expression (11). Recent comparative whole-genome DNA methylation studies shed further light on molecular mechanisms behind MS pathogenesis (9, 13), the vast majority of them focusing on RRMS stage of disease.

In this study, we aimed to examine the molecular changes that associate with MS course. Using a multilayered (genetic, epigenetic, transcriptomic) and cross-tissue (blood, brain) approach in cohorts of MS patients and controls, we demonstrate an interplay between regional genetic variation, DNA methylation and gene expression in the chromosome 1q21.1 region, in PPMS patients specifically. We addressed the link between these three molecular layers using in-vitro reporter gene assays and CRISPR/dCas9 epigenome editing. Our findings suggest that genetically controlled methylation at 1q21.1 locus might contribute to PPMS pathology though transcriptional regulation of proximal genes, particularly *CHD1L*.

Results

Hypermethylation of an intergenic region in the 1q21.1 locus of PPMS patients

We profiled genome-wide DNA methylation in the blood of RRMS, SPMS and rare PPMS patients and matched healthy controls (HC, cohort 1, n = 279, Fig. 1, SI Appendix Table S1), using the Illumina Infinium HumanMethylation450 BeadChip (450K array). After adjustment for confounders, we identified one differentially methylated region (DMR) in PPMS patients in comparison with HC (P = 6.16 x 10^{-6}), RRMS (P = 2.51 x 10^{-6}) and SPMS (P = 7.33 x 10^{-6}) patients (FWER < 0.05, Fig. 2a, SI Appendix Table S2). The DMR, located in an intergenic CG-rich region on chromosome 1 (q21.1): 146549909–146551201 (GRCh37/hg19), consists of 8 consecutive CpG probes displaying hypermethylation in PPMS patients compared to RRMS, SPMS as well as HC (Fig. 2b). Considering the low number of PPMS patients (n = 4), we

selected an independent cohort for replication including 36 PPMS and 48 RRMS patients, matched for gender, age and disease duration (cohort 2, Fig. 1, SI Appendix Table S1). We designed pyrosequencing assays covering seven CpG sites (CpG 1-7), including the 450K probes exhibiting the largest changes cg21263664 (CpG 1), cg03526459 (CpG 3), cg16814483 (CpG 5), cg02487331 (CpG 7) and three additional adjacent CpG sites located between theses 450K-CpGs (Fig. 2a). A total of six out of these seven CpGs were found significantly hypermethylated in PPMS compared to RRMS patients (Fig. 2c). These data imply that PPMS patients display hypermethylation of an intergenic region within the 1q21.1 locus, suggesting a potential involvement in the PPMS pathogenesis.

Methylation of the PPMS-associated 1q21.1 locus is under strong genetic control in the blood and the CNS

Previous studies have revealed a complex interplay between genetic and epigenetic variations by reporting that part of the epigenome is under genetic control in general (14, 15), and more particularly, that genetically dependent DNA methylation can mediate risk to develop MS (11). Interestingly, our data revealed that methylation clustered within three methylation levels (i.e. low, medium and high) in both cohorts (Fig. 2b-c), a pattern typically observed for genetically controlled methylation. To test for potential genetic dependence, we performed genome-wide methylation Quantitative Trait Loci (meQTL) analysis in cohort 1 and found 19 SNPs, located in the extended 1q21.1 locus (-50 kb to +400 kb), associating with methylation levels of the DMR, with strongest effects coming from rs1969869, rs21327, rs647596, rs10900384 and rs12401360 (genotype *vs.* methylation estimate = 0.19, $p < 10^{-16}$) (Fig. 3a, SI Appendix Table S3). To further validate this finding, we conducted locus-specific meQTL analysis in cohort 2 by testing all SNPs covering ± 500 kb window encompassing the DMR against each pyrosequenced CpG. Of note, only eight out of the 19 meQTL-SNPs identified in cohort 1 could be assessed in this cohort. Out of the 123 SNPs tested in cohort 2, two variants showed significant (rs1969869, rs4950357, $p < 10^{-8}$) and two suggestive (rs647596, rs10900384, $p < 10^{-5}$) associations with CpGs methylation (Fig. 3a). An example of genetic control of methylation at CpG 4 (pyrosequenced CpG located between cg03526459 and cg16814483, Fig. 2c) is illustrated in Figure 3b. The two strongest SNPs, rs1969869 and rs4950357, displayed positive association between the minor allele and CpG methylation levels (Fig. 3a, SI Appendix Table S4). In addition to these four SNPs, 66 SNPs demonstrated nominal association with methylation ($p < 0.05$) (SI Appendix Table S4). Overall, all eight overlapping SNPs identified in cohort 1 displayed significant and similar direction of changes also in the cohort 2 (Fig. 3a, SI Appendix Tables S3 and S4). Many of the SNPs with similar effect, i.e. minor allele associating with either high or low methylation, were in strong linkage disequilibrium (LD > 0.8) and were therefore grouped into LD clusters (Fig. 3a).

Our results implying a link between genetic variation and blood DNA methylation at the 1q21.1 region, a locus reported to be crucial for brain size (16, 17) and neuropsychiatric disorders (18-20), posed the question whether such effect might occur in the CNS as well. To address this, we examined putative genetic influences on the methylation at 1q21.1 DMR in the brain using publicly available meQTL data from brain tissue of 543 individuals (15). Results showed that SNPs corresponding to 11 out of 14 SNP clusters demonstrated strong meQTLs in the CNS as well, with similar direction of the effect as observed in the blood (Fig. 3c, SI Appendix Table S5), exemplified for cg02487331 (Fig. 3c). Altogether, these findings strongly suggest that methylation at CpGs in the 1q21.1 DMR are under genetic control in the blood and CNS compartments.

Genetic variants in 1q21.1 predispose for PPMS and associate with methylation and gene expression changes in the CNS

We next asked whether the genetic variation in 1q21.1 also affects the risk of developing PPMS. We tested the association between all the imputed SNPs in the extended locus (3,057 SNPs, chr.1: 145695987- 147526765, hg19) and disease course, comparing PPMS and bout-onset MS (BOMS including RRMS and SPMS) patients in a combined Swedish cohort of 9,850 patients

(PPMS n = 603, BOMS n = 9,247) (cohort 3, Fig. 1, SI Appendix Table S1). A total of 574 SNPs showed evidence for nominal association ($p < 0.05$) with PPMS (SI Appendix Table S6). Globally, these SNPs mapped to 57 of the 69 identified LD blocks. Of note, 13 SNPs belonging to seven different LD blocks remained significant after Bonferroni correction for multiple testing ($p < 7.2 \times 10^{-4}$).

Brain-meQTL data were available for 149/574 SNPs, belonging to 13 LD blocks. The vast majority of them (147/149) showed evidence for meQTLs in the brain. All the protective variants were found to be associated with lower methylation at 1q21.1 DMR, while 7/8 risk variants for PPMS were associated with higher levels of methylation at 1q21.1 DMR in the brain (SI Appendix Table S7). To further reinforce the evidence of a genetic influence at 1q21.1 on the risk of developing PPMS, we conducted a meta-analysis between the aforementioned Swedish cohort and an Italian cohort of PPMS (n = 501) and BOMS (n = 2,088) individuals (2,272 SNPs). A total of 64 SNPs, from 16 different LD blocks, showed a nominal association ($p < 0.05$) and same direction of effect in both cohorts (Table 1, SI Appendix Table S8). Five SNPs, tagging two LD blocks, remained significant after correction for multiple testing accounting for LD blocks ($p < 7.2 \times 10^{-4}$) (Table 1). All the five SNPs were associated with an increased risk of PPMS, and annotation to brain-meQTL data confirmed that they also lead to higher methylation (Fig. 3d, SI Appendix Table S7). These findings suggest a functional link between high methylation at 1q21.1 DMR and the genetic predisposition to develop PPMS.

We next assessed whether the identified genetic variations that associate with PPMS and methylation impact gene expression in the brain tissue. Taking advantage of the GTEx and xQTL serve databases, we found that a large fraction of the variants (mapping to 10/16 and 34/57 LD blocks from the meta-analysis and Swedish cohort, respectively) conditioned transcript levels of neighboring genes within the locus *(PRKAB2*, *CHD1L* and *FMO5),* as well as long non-coding RNAs in the brain (SI Appendix Table S7). As exemplified in Figure 3d, variants predisposing for higher DMR methylation and PPMS risk associated with lower *CHD1L* and *PRKAB2* expression while variants conferring low DMR methylation and PPMS protection associated with higher *CHD1L* and *FMO5* expression and lower *PRKAB2* transcript levels. *CHD1L* gene displayed the most consistent changes regarding the impact of genetic variation on PPMS risk, methylation and *CHD1L* expression. These data connecting the genetic variation, methylation and transcription in the extended 1q21.1 region are consistent with genomic annotations of the DMR underscoring putative regulatory features as well as short-range physical interaction with proximal chromatin segments harboring eQTL genes (SI Appendix Fig. S1). Thus, the variants influencing the risk of developing PPMS and controlling DNA methylation in the 1q21.1 locus likely also exert an effect on the expression of proximal genes in the brain, particularly *CHD1L*, *FMO5* and *PRKAB2*.

Methylation at the 1q21.1 locus regulates proximal gene expression in neuron-like cells

In order to functionally address the causal relationship between epigenetic and transcriptional changes, we first tested whether methylation at the 1q21.1 DMR can exhibit regulatory properties on transcription, as suggested by genomic annotations of the locus (Fig. 2a, SI Appendix Fig. S1), by examining methylation-sensitive enhancer and promoter activity using in-vitro methylation assays. Two distinct 1 kb fragments harboring the DMR sequence, isolated from PPMS patients with low (rs1969869: CC) and high (rs1969869: AA) methylation levels at the identified DMR, were inserted in CpG-free vector-based reporter system. The sequences were subsequently methylated using two different methyltransferases, *M.SssI* enzyme methylating all CpG sites (57 CpGs) and *HhaI* enzyme targeting only internal cytosine residues from the consensus sequence GCGC (7 CpGs). The 3'-5' oriented DNA sequence of both genotypes exhibited potent constitutive promoter activity on the reporter gene (Mock condition), this basal activity being nonetheless halved in carriers of the minor allele compared to AA-homozygotes (Fig. 4a). The DMR manifested enhancer activity as well, although to a lesser extent, with no clear contribution of each allele or sequence orientation (Fig. 4b). Comparison of the unmethylated and methylated sequences revealed a significant reduction of the promoter and enhancer activity when the insert was fully methylated (Fig. 4a-b). Thus, controlling the level of methylation in the DMR region might have the potential regulatory effect on gene expression.

To formally address the impact of DNA methylation on endogenous gene expression, we exploited the CRISPR/dCas9-based epigenome editing platform which allows editing of methylation in a sequence-specific manner in combination with tailored single guide RNA (gRNA). We took advantage of the fact that several cell lines display hypermethylation at the 1q21.1 locus (as annotated by ENCODE Roadmap), mimicking methylation pattern in PPMS patients, and developed constructs expressing deactivated Cas9 fused to the catalytic domain of the demethylating enzyme TET1 (dCas9-TET1) to remove methylation from specific CpGs (see Methods for further description). We could validate the editing efficiency of dCas9-TET1 constructs by targeting 5 CpGs composing *MGAT3* gene promoter, with 10-50% de-methylation as previously reported (21) (SI Appendix Fig. S2). To remove methylation at CpGs of the PPMS-associated DMR, we first designed and functionally screened 9 gRNAs targeting the two 450K probes exhibiting the largest changes (cg21263664, cg03526459) and adjacent CpGs in HEK293T cells (Fig. 4c). Negative controls consisted of cells transfected with a non-targeting (nt) gRNA, the catalytically inactive form of TET1 (TET1-IM) or non-transfected cells. DNA methylation analysis, using pyrosequencing, showed different degrees of de-methylation ranging from 10-50% reduction in methylation at single or multiple CpG sites depending on the gRNA (Fig. 4d). Delivery of dCas9-TET1 together with gRNA2 and gRNA3 could achieve robust demethylation at four sites, including cg03526459, in HEK293T cells (Fig. 4d). We next adapted this strategy to neuroblastoma SH-SY5Y cells using transduction with dCas9-TET1 + gRNA2 + gRNA3 lentiviruses (Fig. 4e) and could confirm the editing efficiency in these cells with 15-35% decrease of DNA methylation spanning throughout CpGs 1-3 (Fig. 4f). We then assessed by qPCR the expression of genes located in the vicinity of the DMR. These include the three coding genes found regulated by the same meQTL-SNPs in the normal brain (Fig. 3c), namely *CHD1L* gene encoding a DNA helicase protein involved in DNA repair, *PRKAB2* gene encoding the non-catalytic subunit of the AMP-activated protein kinase (AMPK), which serves as an energy sensor protein kinase regulating cellular energy metabolism and *FMO5* gene encoding a Baeyer-Villiger monooxygenase implicated in liver function and metabolic ageing (22). The induced de-methylation, even moderate, of CpGs in the 1q21.1 DMR in SH-SY5Y cells resulted in increased expression of *CHD1L* and *PRKAB2* genes while the expression of *FMO5* and other proximal transcripts, *PDIA3P1* and *PFN1P5*, did not vary significantly (Fig. 4g). Of note, we did not observe any significant gene expression changes following dCas9-TET1 co-delivery with single or combined gRNAs in HEK293T cells (SI Appendix Fig. S3).

Collectively, these data suggest that the intergenic PPMS-associated DNA methylation at 1q21.1 region exerts regulatory properties on transcriptional processes. The methylation-mediated regulation of gene expression affects *CHD1L* and *PRKAB2* genes in neuron-like cells.

Network analysis implicates *CHD1L* and *PRKAB2* genes in PPMS brain pathology

To further delineate the putative relevance of the genes included in the 1q21.1 locus in PPMS brain pathology, we constructed an unbiased correlation network analysis using RNA-sequencing-derived gene expression matrix from brain tissue samples of progressive MS patients (n = 12) and non-neurological controls (n = 10) (9) (Fig. 5). After gene-pair permutation and planar filtering, the network consisted of 0.5 million interactions among 27,059 genes (FDR < 0.05) (Fig. 5a). Multiscale clustering analysis further clustered these interactions into 757 non-overlapping modules (Fig. 5b). We then evaluated the relevance of these modules for PPMS (n = 5) and SPMS (n = 7) phenotypic traits by applying cluster trait association analysis (Fig. 5b). Three modules survived statistical testing, one of them (module #1) being correlated to SPMS trait while the two others (modules #2 and #3) showing high significance to PPMS phenotype (Fig. 5b, SI Appendix Table S9). Strikingly, these modules were found centered on genes from the extended 1q21.1 locus. Indeed, exploration of the biggest module (module #2), consisting of 380 nodes and 1079 interactions, revealed *CHD1L* as a central node within this network, closely interacting with six genes of a sub-module (Fig. 5c). Relative centrality could also be observed for the other two modules, which include *FMO5* among 40 nodes (module #1) and *PRKAB2* among 54 nodes (module #3) (Fig. 5c). Of note, *CHD1L* and *PRKAB2* were the only genes from the

extended 1q21.1 locus to partake in the regulatory gene network underlying PPMS brain pathology in our analysis. Gene ontology analysis, using Ingenuity Pathway Analysis, underscored implication of all modules in nervous processes. This is particularly the case for module #2 with terms linked to neuronal functions, while additional *Biological Functions* were found associated to module #1 (e.g. metabolic processes) and module #3 (e.g. cell cycle) (Fig. 5c, SI Appendix Table S10). Thus, findings from unbiased *in-silico* approach support a potential role of genotype-methylation-expression regulatory network affecting genes of chromosome 1q21.1 extended locus, such as *CHD1L* and *PRKAB2,* in CNS processes in PPMS patients.

To verify the network modules, we used large GTEx dataset from healthy individuals (SI Appendix Table S11). We did not detect our networks in any of 14 strata, but *CHD1L*, *FMO5* and *PRKAB2* genes belonged to significantly co-expressed genes networks only in the cortex and tibial nerve. This could indicate that, beyond constitutive expression of these genes in multiple tissues and cells, the existence of the networks is dependent on the disease processes and possibly more restricted to neurons. We thus investigated additional datasets comprising CNS tissue from MS patients, particularly focusing on those in which co-expressed networks containing *CHD1L*, *FMO5* or *PRKAB2* gene were detectable (SI Appendix Table S11).The $CUX2^+$ excitatory neurons, previously shown to be specifically affected in MS, displayed significant co-expression of *CHD1L*, *FMO5* and *PRKAB2* with other genes, thereby forming network modules, in the single nuclei RNA sequencing (snRNA-seq) dataset from the original study (23). We detected a significant overlap of our *CHD1L* module, but not *FMO5* and *PRKAB2* modules, with the $CUX2^+$ specific gene signature (overlapping = 18, p-value = 2.95×10^{-6}, OR = 3.65). Conversely, the *CHD1L* module in $CUX2^+$ neurons significantly overlapped with our *CHD1L* module with shared closest interacting genes and pathways related to neuronal functions (overlapping = 20, p-value = 0.03, OR=1.56, SI Appendix Table S9, SI Appendix Fig. S4).

Discussion

MS is a multifactorial and heterogeneous neurological disease with unpredictable trajectories affecting young individuals. Treatment of progressive forms remains the greatest challenge in the care of MS patients, which is likely due to our partial knowledge of the pathological processes underlying these forms of disease. In this study, we utilized a multi-omics (genetic, epigenetic, transcriptomic) approach in several cohorts, in combination with in-vitro functional experiments and network analysis, to gain more insights into the primary progressive form of MS. We identified a genetically controlled hypermethylated region in the chromosome 1q21.1 locus which might affect the expression of proximal genes, particularly *CHD1L*, in the brain of PPMS patients.

Attempts to identify genetic variants that predispose for PPMS have not yielded reproducible associations with the exception of the known RRMS-risk *HLA-DRB1*15:01* variant (24, 25). One of the challenges of the genetic studies in PPMS is the limited availability of PPMS cases that comprise around 10% of all MS cases. We and others have shown that integrating additional layers of gene regulation, such as DNA methylation, can reveal genetic associations that are difficult to identify using conventional genetic studies (11, 26-28). In this study, we combined methylome profiling with locus-specific genetic association analyses in independent cohorts and identified a genetically controlled DMR in the 1q21.1 locus that displayed hypermethylation in PPMS patients specifically. Since SNPs can affect both CpGs as well as the probe/primer hybridization in methylation assays, we have ensured that DNA methylation measurements are not subject to such technical biases.

The same genetic variants that control methylation and gene expression in the locus associated with PPMS risk, suggesting a functional link between genetic, epigenetic, and transcriptional modalities in 1q21.1 in PPMS patients. We provided evidence for association with the risk of developing PPMS in two independent cohorts from Sweden and Italy comprising 1,104 PPMS cases compared to 11,335 of relapse onset MS, which is the largest reported PPMS cohort to date. Nevertheless, establishing unequivocal genetic association alone would require cohort sizes

that could be challenging to obtain even by large multicentric efforts, further emphasising the need to combine multiple independent layers of evidence.

Our findings should also be considered in the light of the remarkably complex genomic architecture of the 1q21.1 locus displaying considerable copy-number variations. Indeed, the extended 1q21.1 genomic locus covering the identified DMR is characterized by the largest copy number expansion between non-human and human primate lineage, such variation correlating with evolutionary brain size in a dose-dependent manner (16, 17). Copy-number variations in this region have also been associated with brain disorders such cognitive and motor deficits, neuroblastoma, autistic spectrum disorder and schizophrenia (18-20). Our further analysis revealed that some of the SNPs conferring risk for PPMS, are associated with Schizophrenia (29) and are controlling the expression of neighboring genes including *CHD1L* in the brain cells. These associations with brain size and neurodevelopmental disorders further support the idea that inherent brain tissue vulnerability influenced by the genes in the locus may predispose for rapid and progressive MS disease, as recently suggested for the severity of MS (30). Whether the changes identified in the 1q21.1 locus in our study are related to structural variations of the genome warrants further investigation.

The observed dual meQTL and eQTL effects in the CNS tissue, underscore the possible contribution of genetic-epigenetic-transcriptional regulation in PPMS brain pathology. In this context, we found that genetic variation that strongly associated with elevated DNA methylation levels at 1q21.1 and modestly associated with increased PPMS risk is linked to lower expression of *CHD1L* transcript in the CNS. We next sought to formally explore the possibility that DNA methylation may directly influence gene expression. We first demonstrated intrinsic methylation-sensitive promoter and enhancer activity of PPMS-associated DMR sequence using in-vitro methylation assays. We then utilized CRISPR/dCas9-TET1 epigenome editing approach to achieve effective and locus-specific demethylation at CpGs of the identified DMR and found that manipulating DNA methylation at the 1q21.1 DMR affects the expression of the proximal *CHD1L* and *PRKAB2* genes in neuron-like cells, an effect we could not observe in HEK293T cells. These data, together with the indisputable involvement of 1q21.1 region in neuronal circuitry and brain integrity (16-20), implicate genes of the locus in neuropathological processes in PPMS. Undeniably, given the occurrence of meQTL effects in the blood, one cannot exclude a contribution of 1q21.1 regulatory network in the peripheral immune compartment as well. Similar trans-tissue effects with shared pattern between the immune and nervous compartments have previously observed in the context of progressive MS disease (31). Collectively, these findings portray DNA methylation as a putative intermediary of genetic influence on gene expression, particularly in the CNS of PPMS patients.

Our unbiased correlation network analysis of published transcriptomic data obtained from post-mortem brain tissue from PPMS, SPMS patients and controls (9), identified *CHD1L* and *PRKAB2* transcripts as implicated in PPMS specific regulatory gene networks while *FMO5* gene was found significantly connected to SPMS phenotype. *FMO5* encodes for an atypical flavin containing monooxygenase protein with the ability to oxidize a wide range of substrates and xenobiotic, whose disruption has been shown to affect metabolic ageing in rodents (32). *CHD1L* encodes a DNA helicase implicated in chromatin-remodelling during DNA repair, with both depletion and overexpression of CHD1L leading to genomic sensitivity to DNA-damaging agents (33). *PRKAB2* encodes the beta subunit of AMP-activated kinase, a neuroprotective energy-sensing kinase exerting pivotal roles in the cellular energy metabolism required for maintenance of neuronal integrity (34). Accordingly, previous studies on neuron-specific loss of PRKAB2 function fruit flies resulted in progressive fragmentation of dendritic arborisation, cognitive impairment as well as reduced stress resistance and lifespan (34). Interestingly, bulk and single cell transcriptomics in brain tissue have found dysregulation of several genes located within the identified 1q21.1 locus, including *CHD1L*, *PRKAB2*, *FMO5* transcripts along with several members of the *NBPF* family of genes, in progressive MS patients compared to control individuals (9, 23). Markedly, *CHD1L* gene has been identified in the stress-related signature of excitatory CUX2-expressing projection neurons in upper-cortical layers, which are particularly susceptible to degeneration in MS patients (23). Additionally, a large fraction of *CHD1L* (3/6) closest network neighbours identified in our

study were found significantly upregulated in these stressed excitatory neurons as well. Moreover, our *CHD1L* network module displayed a significant overlap, both on the gene and pathway level, with the transcriptional signature of $CUX2^+$ neurons as well as the *CHD1L* network detected in $CUX2^+$ neurons using snRNA-seq dataset from Schirmer et *al.* (23). It is therefore reasonable to speculate on the involvement of *CHD1L* in the compensatory mechanisms counteracting the cellular burden, e.g. genomic and metabolic stress, observed in these neurons, although validation in large PPMS dataset is warranted. More specifically, genetic predisposition to high methylation and low expression of *CHD1L* gene might influence susceptibility to PPMS by limiting the inherent repair capacity in the brain.

In conclusion, our study suggests that PPMS patients display distinct molecular changes compared to SPMS, RRMS and healthy individuals. The data further support the hypothesis of a causal genetic-epigenetic-transcriptional interplay within the extended 1q21.1 locus, with functional evidence of contribution from *CHD1L* in progressive MS pathology. Given the reversible nature of DNA methylation, our findings open new avenues for development of therapeutic strategies, such as the targeted epigenetic therapy, in the treatment of progressive MS.

Materials and Methods

Cohorts

Details of the cohorts are described in the SI Appendix Table S1. Briefly, for genome-wide DNA methylation and methylation quantitative trait locus (meQTL) analysis used in cohort 1, peripheral blood samples were collected form 140 MS, patients including 120 RRMS, 4 PPMS and 16 SPMS patients, and 139 healthy individuals (HC), as previously described (11). An independent cohort, cohort 2, consisting of 48 RRMS and 36 PPMS patients (matched for age, sex, disease duration and Swedish descent) was used for pyrosequencing validation and locus-specific meQTL analysis (35). Cohort 3 and the additional Italian cohort used for genetic association study comprises 1,104 PPMS and 11,335 BOMS, as described in the corresponding sections below. Gene expression data (RNA-sequencing) from bulk brain tissue samples of progressive MS patients (5 PPMS and 7 SPMS) and non-neurological controls (n = 10), previously described (9), were used for correlation network analysis and validation was performed in neuronal snRNA-seq data (23). Additionally, we utilized publicly available databases from xQTL serve (15) (n = 543 bulk prefrontal cortex samples, http://mostafavilab.stat.ubc.ca/xQTLServe/) and GTEx (selecting all available nervous tissues, https://gtexportal.org/) platforms to address meQTL and eQTL effects in the CNS. No sample size calculation was performed for the cohorts involved in this study.

Ethics approval and consent to participate

All experiments on human subjects were approved by the Regional Ethical Review Board in Stockholm and carried out in accordance with institutional guidelines. Written informed consent was obtained from all study participants.

Genome-wide DNA methylation and meQTL analyses (cohort 1)

DNA methylation analysis. The methylation data from Infinium HumanMethylation450 (450K) arrays was preprocessed as previously described (11) and in supporting information using the Illumina default procedure implemented in the Bioconductor minfi package (36) To identify differentially methylated regions (DMRs) associated with the PPMS phenotype, we used the bumphunter function in minfi package (36) with adjustment for confounders: age, sex, self-reported smoking status (ever smokers vs. never smokers), hybridization date, and the first two principle components of estimated differential cell counts. Region that has a family wise error rate

(FWER) less than 0.05 with 1000 resamples and contains at least 2 probes was identified as a trait-associated DMR.

Methylation QTL analysis. To identify potential genetic dependency, the PPMS-associated DMR was tested for association with genotype (594,262 SNPs) using an additive minor-allele dosage model. Genotype-DMR associations were corrected for multiple testing using a stringent Bonferroni-adjusted threshold of 0.05.

Locus-specific DNA methylation and meQTL analyses (cohort 2)

DNA methylation analysis. For validation of the identified PPMS-associated DMR, pyrosequencing analysis of 7 CpG sites in the locus was performed as detailed in supporting information and SI Appendix Table S12, SI Appendix Figure S5.

Methylation QTL analysis. Methylation data was RANK transformed in R using R Core team (Vienna, Austria, https://www.R-project.org/). Genotyping was carried out at deCODE (deCODE genetics/Amgen, Reykjavik, Iceland) using Illumina OmniExpress chip with 716,503 SNPs mapped to the Human Assembly Feb.2009 (GRCh37/hg19). Of 84 individuals, 83 where genotyped in deCODE and 82 of them passed QC. We performed meQTL analysis of chromosome 1 from bp 146500000 to bp 147000000, in PLINK (37) excluding SNPs with less than 98% genotyping rate and SNPs that were not in Hardy-Weinberg equilibrium ($p < 0.05$) and corrected for 5 population based (ancestral informative markers) principal component analysis covariates. After quality control, 123 SNPs remained in the region. Genotype-CpG associations were corrected for multiple testing using stringent Bonferroni-adjusted threshold of 0.05.

Genetic association study in the Swedish (SWE) cohort

Patients from the Swedish (SWE) cohort were genotyped in two different batches at deCODE Genetics using Illumina Human OmniExpress 24 v1 (OE) and Global Screening Array MD 24 v2 (GSA) arrays, following manufacturer's instructions. For the genetic association analysis we extracted all the imputed SNPs (n = 3,057) in the extended chr1 locus (from bp 146500000 to bp 147000000). A total of 7,682,164 autosomal variants passed quality controls and were tested for SNP-to-phenotype association (PPMS = 603 versus BOMS = 9,247) in the generalized linear model analysis including covariates, separately for individuals genotyped on OE chip and those genotyped on GSA arrays (see details in supporting information). Subsequently, the results from the two independent association studies (OE and GSA) were meta-analyzed using fixed-effect and random-effect models as implemented in PLINK. Sixty-nine LD blocks were identified and used in a Bonferroni correction to account for multiple testing.

Genetic association study in the Italian (ITA) cohort

For the Italian cohort, patients were recruited at the Laboratory of Human Genetics of Neurological Disorders at the San Raffaele Scientific Institute in Milan, Italy and genotyped on Illumina platforms. After quality controls (see supporting information), a logistic regression model, as described for the SWE cohort, was used to study the association between the SNPs in the extended chr1 locus and the course of MS in a total of 2,589 patients (PP = 501; BOMS = 2,088). Sex and PC 1 to 8 were used as covariates in the model.

SWE and ITA meta-analysis

A fixed-effect model meta-analysis of the standard errors of the odds ratio, as implemented in Plink (38), was applied on the three cohorts. The number of common variants in all the cohorts was 2,676. Multiple testing issue was addressed as described for the SWE cohort (see also supporting information).

In-vitro methylation assay

To address the regulatory features of the identified DMR, we used in-vitro DNA methylation reporter assay. A 927 bp fragment encompassing the identified DMR was amplified using blood genomic DNA from PPMS patients presenting with low (rs1969869: CC) and high (rs1969869: AA) methylation levels at the identified DMR. The amplified products in direct and reverse orientation were inserted into pCpG-free promoter vector (Invivogen) containing a Lucia luciferase reporter and into a pCpG-free basic vector (Invivogen) containing a murine secreted embryonic alkaline phosphatase (mSEAP) reporter gene for assessment of enhancer and promoter activity, respectively. After complete, partial or mock methylation of the constructs and transfection of HEK293T cells, Lucia or SEAP signals were normalized against Renilla (triplicate) and experiments were replicated at least two times. Details are provided in supporting information.

CRISPR/dCas9-TET1 epigenome editing

dCas9-TET1 and gRNA generation. To address dCas9-TET1-mediated epigenome editing in SH-SY5Y cell line, we utilized the lentivirus version of the cassettes. Detailed methods to engineer the P3-dCas9-Tet1-GFP-Puro (Addgene #190728), P3-Lenti-dCas9-Tet1-GFP (Addgene #190729) and P3-Lenti-dCas9-Tet1IM-GFP (Addgene #190730) constructs are available in supporting information. Details and maps of the final constructs used in this study are presented in SI Appendix Figure S7. All gRNAs were designed by CRISPOR Version 4.98 (39) both on the sense and antisense strands, with sequence and mapping presented in the SI Appendix Table S12 and SI Appendix Fig. S8.

dCas9-TET1 delivery to HEK293T and SH-SY5Y cells. To test the efficiency of epigenome editing, we exploited HEK293T ease of transfection and performed gRNAs screen. Different gRNAs were transfected either individually or in combination based on the target site, using Lipofectamine 3000 (Invitrogen). For all experiments both on HEK293T and SH-SY5Y cells, DNA was extracted after 72 hours and bisulfite conversion was performed using 200 ng of the extracted DNA (BS-DNA, EZ DNA methylation kit, ZYMO research). DNA methylation was assessed using pyrosequencing, as described above. For all experiments conducted on SH-SY5Y cells, we delivered a mix of the two gRNAs that showed the highest efficiency in reducing methylation in HEK293T cells (gRNA #2 and #3). Lentiviruses generation and subsequent transduction of SH-SY5Y cells are performed based on the standard protocols which details are available in supporting information.

qPCR analysis

Total RNA and DNA were extracted using AllPrep DNA/RNA Kits (Qiagen) according to the manufacture instruction. RNA and DNA concentrations and quality were verified by QIAxpert (Qiagen). Reverse transcription of RNA was performed using the manufacturer's instructions of iScript™ cDNA Synthesis Kit (Bio-Rad Laboratories, Inc., CA). Real-time PCR was performed on a BioRad CFX384 Touch Real-Time PCR Detection System using iQ™ SYBR® Green Supermix (Bio-Rad Laboratories, Inc., CA) in a standard three step PCR protocol. The relative expressions of the selected genes were normalized to the reference gene *GAPDH*. The specificity of real time PCR reaction was verified by the melt curve analysis. The expression level of selected genes were analyzed using ΔΔCT method (40) and compared via independent t-test. All statistical analyses were performed in GraphPad Prism 6 and 7 (GraphPad Software).

Correlation network analysis in MS brain

Raw data analysis. The fastq files corresponding to bulk gene expression (RNA-sequencing) data from brain tissue samples of progressive MS patients (n = 12) and non-neurological controls (n = 10) (9, 23) were extracted from the RAW RNA sequence files and checked for quality control using multiqc software to make them ready for alignment (41). After trimming using the trimgalore program (42), fastqc files were aligned and annotated using STAR aligner and Stringtie software (43) by applying human hg38 refseq information from UCSC. The analysis was performed on the extracted count matrix using bash and Python.

Network analysis. In order to utilize a brain-specific network module, we applied a previously established bioinformatic pipeline utilizing co-expression network analysis (44), as described in supporting information. The final network consisted of 0.5 million interactions among 27,059 expressed genes which clustered into 757 non-overlapping modules. For the validation data, we applied the same pipeline on several datasets (SI Appendix Table S11). In the $CUX2^+$ neuronal snRNA-seq count data (23), planar maximal filtration of the Spearmen correlated network of 10780 genes was multiscale clustered using the MEGENA package in R. This resulted in 91 modules out of which 1 module with *CHD1L* was significant and was further analyzed with Fisher enrichment test and pathway analysis using clusterProfiler.

Cluster Trait association analysis. Principal component analysis (PCA) is first performed for each cluster. Next, correlation between the first principal component and each trait was computed as cluster relevance to the trait. The 757 clusters identified from the correlation network were evaluated for the relevance to PPMS, SPMS and control phenotypes. Three clustered passed FDR P-value < 0.05.

Availability of data and materials

The 450K array methylome data generated from whole blood (cohort 1) are available in the Gene Expression Omnibus (GEO) database under accession number GSE106648. The RNA-sequencing data used for correlation network analysis in MS brain are accessible under the accession numbers GSE174647, GSE118257, GSE179427, PRJNA544731 with details presented in Supplementary Table S11. Results from the genetic association analysis (cohort 3) are available in SI Appendix Tables. Due to the GDPR regulations, we cannot deposit any personal information including genetic data, which can be shared upon request and under a Data Access Agreement.

Acknowledgments and funding sources

This study was supported by grants from the Swedish Research Council, the Swedish Association for Persons with Neurological Disabilities, the Swedish Brain Foundation, the Swedish MS Foundation, the Stockholm County Council - ALF project, the European Union's Horizon 2020 research, innovation programme (grant agreement No 733161) and the European Research Council (ERC, grant agreement No 818170), the Knut and Alice Wallenberg Foundation, Hedlund Foundation, Åke Wiberg Foundation and Karolinska Institute's funds. LK is supported by a fellowship from the Margaretha af Ugglas Foundation. MPK is supported by McDonald Fellowship from Multiple Sclerosis International Federation (MSIF) and the EU/EFPIA/OICR/McGill/KTH/Diamond Innovative Medicines Initiative 2 Joint Undertaking (EUbOPEN grant agreement No 875510). CSC is supported by the Blanceflor Boncompagni Ludovisi, née Bildt Foundation. PC is supported by NIH R35-NS111604. The funders of the study had no role in study design, sample acquisition, data collection, data analysis, data interpretation or writing of the manuscript. We are grateful to all volunteers for contributing to the study. We thank Maria Kalomoiri, Jessica Aguilar and Jacqueline Hammer for their help in experimental setup, Dr. Ewoud Ewing for statistics assistance, Dr. Alexander Espinosa for providing plasmid construct and Prof. Lucas Schirmer for providing the $CUX2^+$ specific data. We acknowledge

KIGene facility at the Center for Molecular Medicine and Karolinska Institutet for Sanger sequencing service. The computations were enabled by resources provided by the Swedish National Infrastructure for Computing (SNIC) through Uppsala Multidisciplinary Center for Advanced Computational Science (UPPMAX), partially funded by the Swedish Research Council through grant agreement no. 2018-05973. We thank deCODE for genotyping of the Swedish population (https://www.decode.com/).

References

1. A. Kutzelnigg *et al.*, Cortical demyelination and diffuse white matter injury in multiple sclerosis. *Brain* **128**, 2705-2712 (2005).
2. R. M. Ransohoff, D. A. Hafler, C. F. Lucchinetti, Multiple sclerosis—a quiet revolution. *Nature Reviews Neurology* **11**, 134-142 (2015).
3. D. H. Miller, S. M. Leary, Primary-progressive multiple sclerosis. *The Lancet Neurology* **6**, 903-912 (2007).
4. D. H. Mahad, B. D. Trapp, H. Lassmann, Pathological mechanisms in progressive multiple sclerosis. *Lancet Neurol* **14**, 183-193 (2015).
5. A. J. Thompson, Challenge of progressive multiple sclerosis therapy. *Curr Opin Neurol* **30**, 237-240 (2017).
6. L. Alfredsson, T. Olsson, Lifestyle and environmental factors in multiple sclerosis. *Cold Spring Harbor perspectives in medicine* **9**, a028944 (2019).
7. E. Ewing *et al.*, Combining evidence from four immune cell types identifies DNA methylation patterns that implicate functionally distinct pathways during Multiple Sclerosis progression. *EBioMedicine* **43**, 411-423 (2019).
8. M. C. Graves *et al.*, Methylation differences at the HLA-DRB1 locus in CD4+ T-Cells are associated with multiple sclerosis. *Mult Scler* **20**, 1033-1041 (2014).
9. J. L. Huynh *et al.*, Epigenome-wide differences in pathology-free regions of multiple sclerosis-affected brains. *Nat Neurosci* **17**, 121-130 (2014).
10. L. Kular *et al.*, Neuronal methylome reveals CREB-associated neuro-axonal impairment in multiple sclerosis. *Clin Epigenetics* **11**, 86 (2019).
11. L. Kular *et al.*, DNA methylation as a mediator of HLA-DRB1*15:01 and a protective variant in multiple sclerosis. *Nat Commun* **9**, 2397 (2018).
12. L. Kular *et al.*, DNA methylation changes in glial cells of the normal-appearing white matter in Multiple Sclerosis patients. *Epigenetics*, 1-20 (2022).
13. S. D. Bos *et al.*, Genome-wide DNA methylation profiles indicate CD8+ T cell hypermethylation in multiple sclerosis. *PloS one* **10**, e0117403 (2015).
14. L. Chen *et al.*, Genetic drivers of epigenetic and transcriptional variation in human immune cells. *Cell* **167**, 1398-1414. e1324 (2016).
15. B. Ng *et al.*, An xQTL map integrates the genetic architecture of the human brain's transcriptome and epigenome. *Nat Neurosci* **20**, 1418-1426 (2017).
16. L. J. Dumas *et al.*, DUF1220-domain copy number implicated in human brain-size pathology and evolution. *Am J Hum Genet* **91**, 444-454 (2012).
17. F. Zimmer, S. H. Montgomery, Phylogenetic Analysis Supports a Link between DUF1220 Domain Number and Primate Brain Expansion. *Genome Biol Evol* **7**, 2083-2088 (2015).
18. S. J. Diskin *et al.*, Copy number variation at 1q21.1 associated with neuroblastoma. *Nature* **459**, 987-991 (2009).
19. R. Bernier *et al.*, Clinical phenotype of the recurrent 1q21.1 copy-number variant. *Genet Med* **18**, 341-349 (2016).
20. D. Mehta *et al.*, Comprehensive survey of CNVs influencing gene expression in the human brain and its implications for pathophysiology. *Neurosci Res* **79**, 22-33 (2014).
21. G. Josipovic *et al.*, Antagonistic and synergistic epigenetic modulation using orthologous CRISPR/dCas9-based modular system. *Nucleic Acids Res* **47**, 9637-9657 (2019).
22. S. G. G. Malagon *et al.*, The phenotype of a knockout mouse identifies flavin-containing monooxygenase 5 (FMO5) as a regulator of metabolic ageing. *Biochemical pharmacology* **96**, 267-277 (2015).
23. L. Schirmer *et al.*, Neuronal vulnerability and multilineage diversity in multiple sclerosis. *Nature* **573**, 75-82 (2019).

24. C. International Multiple Sclerosis Genetics *et al.*, Genetic risk and a primary role for cell-mediated immune mechanisms in multiple sclerosis. *Nature* **476**, 214-219 (2011).
25. F. Martinelli-Boneschi *et al.*, A genome-wide association study in progressive multiple sclerosis. *Mult Scler* **18**, 1384-1394 (2012).
26. Y. Liu *et al.*, Epigenome-wide association data implicate DNA methylation as an intermediary of genetic risk in rheumatoid arthritis. *Nature biotechnology* **31**, 142-147 (2013).
27. A. H. Olsson *et al.*, Genome-wide associations between genetic and epigenetic variation influence mRNA expression and insulin secretion in human pancreatic islets. *PLoS genetics* **10**, e1004735 (2014).
28. X. Hong *et al.*, Genome-wide association study identifies peanut allergy-specific loci and evidence of epigenetic mediation in US children. *Nature communications* **6**, 1-12 (2015).
29. V. Trubetskoy *et al.*, Mapping genomic loci implicates genes and synaptic biology in schizophrenia. *Nature* **604**, 502-508 (2022).
30. S. Baranzini, S. Sawcer, I. M. S. G. Consortium, M. Consortium, Genetic analysis of multiple sclerosis severity identifies a novel locus and implicates CNS resilience as a major determinant of outcome. (2022).
31. L. Kular, M. Jagodic, Epigenetic insights into multiple sclerosis disease progression. *J Intern Med* **288**, 82-102 (2020).
32. S. G. Gonzalez Malagon *et al.*, The phenotype of a knockout mouse identifies flavin-containing monooxygenase 5 (FMO5) as a regulator of metabolic ageing. *Biochem Pharmacol* **96**, 267-277 (2015).
33. D. Ahel *et al.*, Poly(ADP-ribose)-dependent regulation of DNA repair by the chromatin remodeling enzyme ALC1. *Science* **325**, 1240-1243 (2009).
34. S. Nagy *et al.*, AMPK signaling linked to the schizophrenia-associated 1q21.1 deletion is required for neuronal and sleep maintenance. *PLoS Genet* **14**, e1007623 (2018).
35. A. K. Hedström, J. Hillert, T. Olsson, L. Alfredsson, Smoking and multiple sclerosis susceptibility. *European journal of epidemiology* **28**, 867-874 (2013).
36. M. J. Aryee *et al.*, Minfi: a flexible and comprehensive Bioconductor package for the analysis of Infinium DNA methylation microarrays. *Bioinformatics* **30**, 1363-1369 (2014).
37. S. Purcell *et al.*, PLINK: a tool set for whole-genome association and population-based linkage analyses. *Am J Hum Genet* **81**, 559-575 (2007).
38. C. C. Chang *et al.*, Second-generation PLINK: rising to the challenge of larger and richer datasets. *Gigascience* **4**, s13742-13015-10047-13748 (2015).
39. J. P. Concordet, M. Haeussler, CRISPOR: intuitive guide selection for CRISPR/Cas9 genome editing experiments and screens. *Nucleic Acids Res* **46**, W242-W245 (2018).
40. K. J. Livak, T. D. Schmittgen, Analysis of relative gene expression data using real-time quantitative PCR and the 2− ΔΔCT method. *methods* **25**, 402-408 (2001).
41. P. Ewels, M. Magnusson, S. Lundin, M. Kaller, MultiQC: summarize analysis results for multiple tools and samples in a single report. *Bioinformatics* **32**, 3047-3048 (2016).
42. Z. Wu, X. Wang, X. Zhang, Using non-uniform read distribution models to improve isoform expression inference in RNA-Seq. *Bioinformatics* **27**, 502-508 (2011).
43. M. Pertea *et al.*, StringTie enables improved reconstruction of a transcriptome from RNA-seq reads. *Nat Biotechnol* **33**, 290-295 (2015).
44. W.-M. Song, B. Zhang, Multiscale embedded gene co-expression network analysis. *PLoS computational biology* **11**, e1004574 (2015).

Figures and Tables legends

Figure 1. Workflow of the study.

MS, multiple sclerosis; PPMS, primary progressive MS; SPMS, secondary progressive MS; RRMS, relapsing-remitting MS; SNP, single nucleotide polymorphism, meQTL and eQTL, methylation and expression quantitative trait loci. SWE, Swedish cohort; ITA, Italian cohort; META, meta-analysis of the SWE and ITA cohorts.

Figure 2. Hypermethylation of the 1q21.1 locus in primary progressive multiple sclerosis patients.

a. Genomic annotation of the identified differentially methylated region (DMR) in 1q21.1, including 450K and pyrosequenced CpG probes and regulatory features, i.e. CpG island (CGI) and chromatin state segmentation by hidden Markov model (ChromHMM) from ENCODE/Broad. **b**. Dot plot and violin plot of DNA methylation differences at the identified DMR on chromosome 1: 146549909-146551201 (hg19) in PPMS (n = 4) compared to RRMS (n = 120), SPMS (n = 16) and HC (n = 139), obtained using Illumina 450K in cohort 1. **c**. Replication of methylation at 7 CpGs (CpG 1-7, including four 450K probes) in an independent cohort (RRMS n = 48, PPMS n = 36) using pyrosequencing. * and ** correspond to P-value < 0.5 and 0.01, respectively, using non-parametric Mann-Whitney U test. MS, multiple sclerosis; PPMS, primary progressive MS; RRMS, relapsing-remitting MS; SPMS, secondary progressive MS; HC, healthy controls; DNase HS, DNase I hypersensitive sites; Txn factor ChIP, Transcription Factor chromatin immunoprecipitation.

Figure 3. Genetic control of methylation and gene expression in the 1q21.1 locus.
a. Genomic and functional annotation of the methylation-controlling variants (SNPs). Linkage disequilibrium (LD) is indicated by shades of red (increasing R^2 from light to dark red) and clustering of SNPs is based on high LD between SNPs ($R^2 > 0.8$). The effects of SNPs on DMR methylation and PPMS risk are depicted using colored circles: the size and color of circles represent significance (–log10 P-value) and direction of the effect, respectively, conferred by the minor allele. Gene location and regulatory features, i.e. CpG island (CGI) and chromatin state segmentation by hidden Markov model (ChromHMM), from ENCODE/Broad. **b**. Association between genetic variation at the extended locus (upper panel) and DNA methylation in blood at CpG 4 of the 1q21.1 DMR, obtained using meQTL analysis in cohort 2 (n=82). Significance is represented as –log10 (P-value). Association of the two strongest variants rs1969869 and rs4950357 with CpG 4 (as an example) are depicted in the lower panel. **c**. Effects of SNPs within each SNP cluster on DNA methylation at 1q21.1 DMR in the brain (using xQTL serve platform (15)) with only significant associations are displayed in colors, blue and red colors representing negative and positive effect of the minor allele, respectively (left panel) and association between genetic variation in the extended locus and DNA methylation at cg02487331 (CpG7) (right panel). The location and code for the CpG numbers is presented in Figure 2c. Significance is represented as –log10 (P-value). *Indicates that the SNPs are in strong LD with rs21327 (LD = 0.7). **d**. Association between genetic variation, DNA methylation (using xQTL serve platform (15)) and gene expression (using GTEx database) in the extended locus for SNPs tagging four variants displaying significant association with PPMS in the meta-analysis of Swedish (SWE) and Italian (ITA) cohorts. Protective and risk genetic effects are depicted in green and orange, respectively. Green and orange colors reflect protective and risk effect on PPMS risk conferred by the genetic variants. Blue and red colors represent negative and positive effect of the minor allele, respectively, on methylation or expression. The data shown in this figure are available in SI Appendix Tables.

Figure 4. Functional impact of methylation at the 1q21.1 DMR on gene expression.

a-b. Promoter (**a**) and enhancer (**b**) activity of the DMR, using CpG-free promoter-free (SEAP) and promoter-containing (Lucia) reporter gene vectors, respectively. Constructs in direct or inverted orientation of DNA segments derived from individual varying according to the genotype at rs1969869 were partially or fully methylated using *HhaI* and *M.SssI* enzymatic treatment, respectively. Results show relative activity (Lucia or SEAP normalized against Renilla) using three replicates in a representative experiment performed at least two times (2-way ANOVA test with Bonferroni correction for multiple comparisons (± SD)). **c**. Schematic representation of the experimental design for gRNAs screen in HEK293T cells including the features of the constructs and gRNA locations. **d**. Heatmap of the DNA methylation levels in successfully transfected (GFP positive) HEK293T cells three days following co-transfection of dCas9-TET1 with single or combined gRNAs in comparison to control conditions, deactivated TET1 (TET1-IM), non-targeting gRNA (ntgRNA) and non-transfected cells. **e**. Schematic representation of the experimental design for functional investigation in SH-SY5Y cells. **f**. DNA methylation levels in SH-SY5Y cells following delivery of dCas9-TET1-, gRNA2- and gRNA3-containing lentiviruses. Methylation percentages represent the average methylation levels of three experiments. **g**. Experiment showing expression of *CHD1L*, *PRKAB2*, *PDIA3P1* and *FMO5* genes relative to *GAPDH* transcript levels, quantified using RT-qPCR. The expression levels represent the average of three experiments (Two-tailed Student's t test (± SD)). ****=p<0,0001, n.s = non-significant.

Figure 5. Implication of *CHD1L* and *PRKAB2* genes in PPMS brain pathology.

a. Schematic representation of the correlation network analysis using bulk MS brain transcriptome(9). The different steps are depicted from left to right: correlation matrix containing gene-gene pairwise Spearman correlations; illustration of the permutation test filtered correlation network surviving an FDR P-value < 0.05 and the planar maximally filtering to convert the scale free network to be able to overlay on a plane spherical surface, reducing the network to 0.5 million interactions among 27509 genes and, finally; representation of the multiscale clustering of the network resulting into 757 non-overlapping clusters. **b**. Heatmap of the correlation coefficients of all 757 non-overlapping modules (left) and the three modules surviving correlation FDR P-value < 0.05 (right) to each tested phenotypic trait, with red gradient colors representing negative (not significant) to positive (significant) correlation. **c**. Representation of the three modules (left), the closest neighbors to candidate genes in each module (middle) and Gene Ontology findings, i.e. *Disease and Biological functions,* obtained using Ingenuity Pathway Analysis. MS, multiple sclerosis; PPMS, primary progressive MS; SPMS, secondary progressive MS; NNC, non-neurological controls.

Table 1. A meta-analysis of genetic association studies with PPMS (n = 1,104) in comparison to BOMS (n = 11,335).

					Meta-analysis		SWE (n = 9,850)		ITA (n = 2,589)	
SNP[a]	**BP**	**CHR**	**LD#**	**A1**	***P***	**OR**	***P***	**OR**	***P***	**OR**
rs900347	145726727	1	1	A	0.0285	0.90	0.0352	0.87	0.3624	0.94
rs11800992	146501783	1	2	A	0.0093	0.82	0.0260	0.78	0.1399	0.85
rs72691008	146708291	1	3	A	0.0017	0.69	0.0083	0.69	0.0895	0.70
rs7514808	146570076	1	4	A	0.0286	0.89	0.0367	0.86	0.3632	0.93
rs72706463	146615555	1	5	A	0.0458	1.29	0.1141	1.37	0.2002	1.24
rs10453880	146693689	1	6	T	0.0065	1.26	0.1083	1.21	0.0236	1.32
rs145465008	146630173	1	7	C	0.0293	1.51	0.4867	1.17	0.0048	2.54
rs115153075	146978424	1	8	T	0.0006	1.48	0.0058	1.42	0.0303	1.74
rs12096043	147060953	1	9	T	0.0001	1.84	0.0005	2.03	0.0633	1.58
rs672619	147058575	1	10	T	0.0013	1.34	0.0374	1.32	0.0146	1.35
rs10494248	147108260	1	11	A	0.0079	1.72	0.0270	1.68	0.1386	1.82
rs140566115	147126437	1	12	A	0.0244	1.53	0.0335	1.66	0.3586	1.34
rs116430961	147312516	1	13	C	0.0101	1.62	0.1335	1.44	0.0265	1.93
rs61740912	147313970	1	14	G	0.0012	1.86	0.0098	1.81	0.0483	1.97
rs112044341	147317235	1	15	A	0.0193	1.47	0.0577	1.46	0.1707	1.49
rs74123747	147382534	1	16	T	0.0496	1.27	0.2194	1.20	0.0813	1.50

PPMS, primary progressive MS; BOMS, bout-onset MS (RRMS + SPMS); OR, odds ratio; LD#, linkage disequilibrium block, SWE, Swedish cohort; ITA, Italian cohort; CHR, Chromosome; *P*, *P*-Value; A1, effect allele; BP, base pair (GRCh37/hg19).
[a]SNP ID highlighted in bold remain significant after Bonferroni correction for multiple testing ($p < 7.2 \times 10^{-4}$).

Figure 1

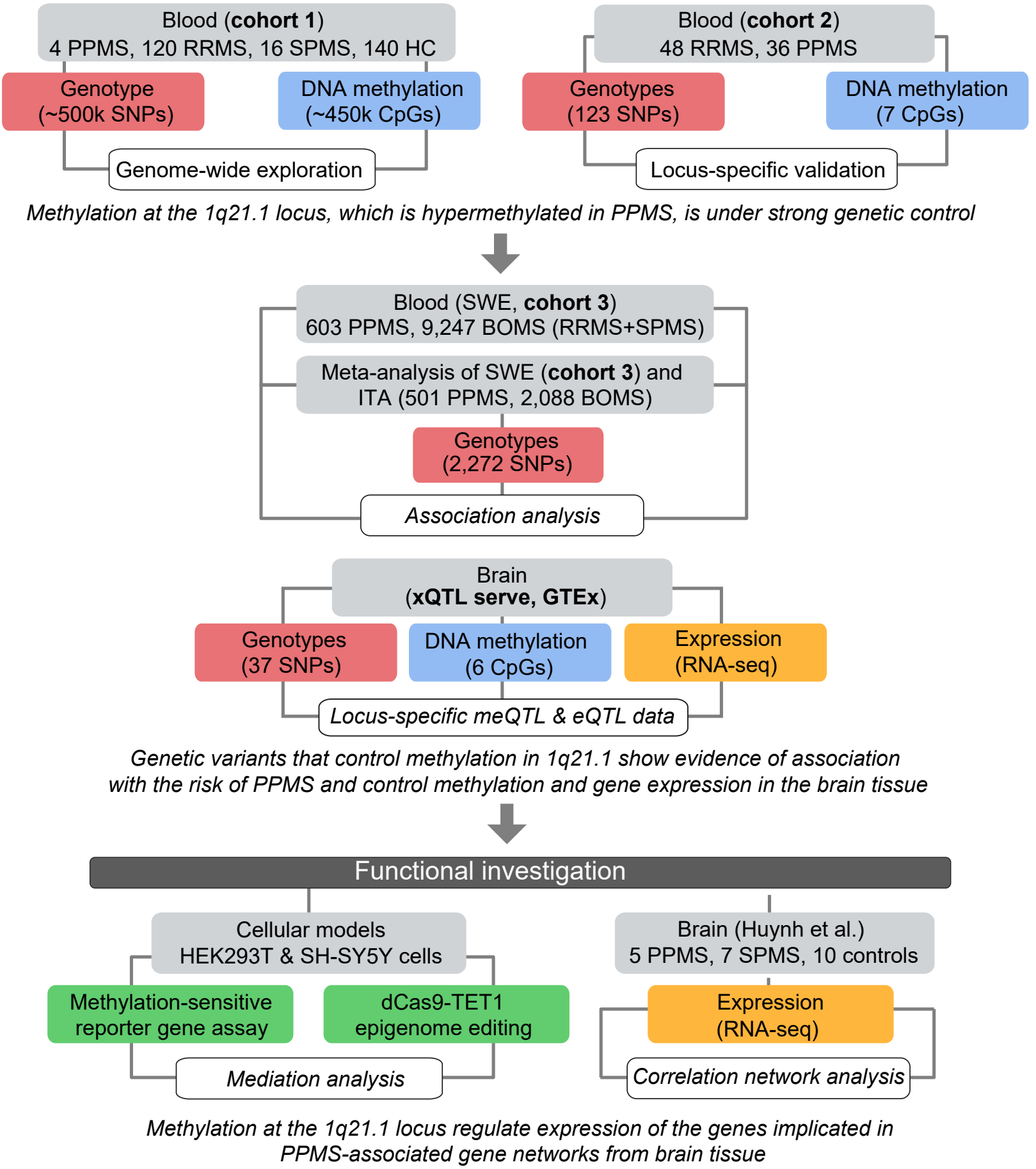
Blood (cohort 1)
4 PPMS, 120 RRMS, 16 SPMS, 140 HC
Genotype (~500k SNPs)
DNA methylation (~450k CpGs)
Genome-wide exploration
Blood (cohort 2)
48 RRMS, 36 PPMS
Genotypes (123 SNPs)
DNA methylation (7 CpGs)
Locus-specific validation
Methylation at the 1q21.1 locus, which is hypermethylated in PPMS, is under strong genetic control
Blood (SWE, cohort 3)
603 PPMS, 9,247 BOMS (RRMS+SPMS)
Meta-analysis of SWE (cohort 3) and ITA (501 PPMS, 2,088 BOMS)
Genotypes (2,272 SNPs)
Association analysis
Brain (xQTL serve, GTEx)
Genotypes (37 SNPs)
DNA methylation (6 CpGs)
Expression (RNA-seq)
Locus-specific meQTL & eQTL data
Genetic variants that control methylation in 1q21.1 show evidence of association with the risk of PPMS and control methylation and gene expression in the brain tissue
Functional investigation
Cellular models
HEK293T & SH-SY5Y cells
Methylation-sensitive reporter gene assay
dCas9-TET1 epigenome editing
Mediation analysis
Brain (Huynh et al.)
5 PPMS, 7 SPMS, 10 controls
Expression (RNA-seq)
Correlation network analysis
Methylation at the 1q21.1 locus regulate expression of the genes implicated in PPMS-associated gene networks from brain tissue

Figure 2

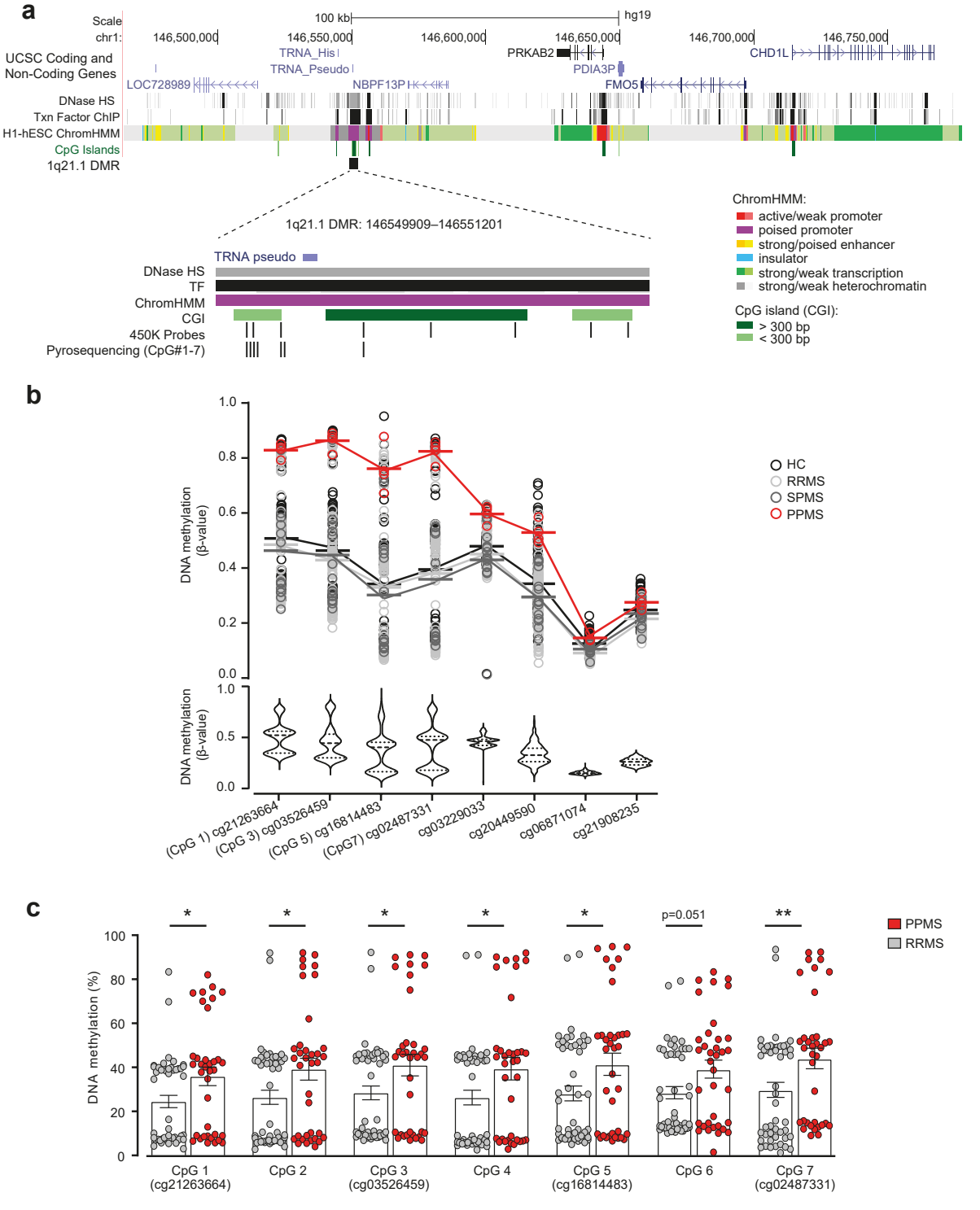
a
Scale
chr1:
100 kb
hg19
146,500,000
146,550,000
146,600,000
146,650,000
146,700,000
146,750,000
UCSC Coding and Non-Coding Genes
TRNA_His
TRNA_Pseudo
PRKAB2
CHD1L
PDIA3P
LOC728989
NBPF13P
FMO5
DNase HS
Txn Factor ChIP
H1-hESC ChromHMM
CpG Islands
1q21.1 DMR
1q21.1 DMR: 146549909–146551201
TRNA pseudo
DNase HS
TF
ChromHMM
CGI
450K Probes
Pyrosequencing (CpG#1-7)
ChromHMM:
active/weak promoter
poised promoter
strong/poised enhancer
insulator
strong/weak transcription
strong/weak heterochromatin
CpG island (CGI):
> 300 bp
< 300 bp
b
DNA methylation (β-value)
1.0
0.8
0.6
0.4
0.2
0.0
0.5
HC
RRMS
SPMS
PPMS
(CpG 1) cg21263664
(CpG 3) cg03526459
(CpG 5) cg16814483
(CpG7) cg02487331
cg03229033
cg20449590
cg06871074
cg21908235
c
DNA methylation (%)
100
80
60
40
20
0
*
**
p=0.051
PPMS
RRMS
CpG 1 (cg21263664)
CpG 2
CpG 3 (cg03526459)
CpG 4
CpG 5 (cg16814483)
CpG 6
CpG 7 (cg02487331)

Figure 3

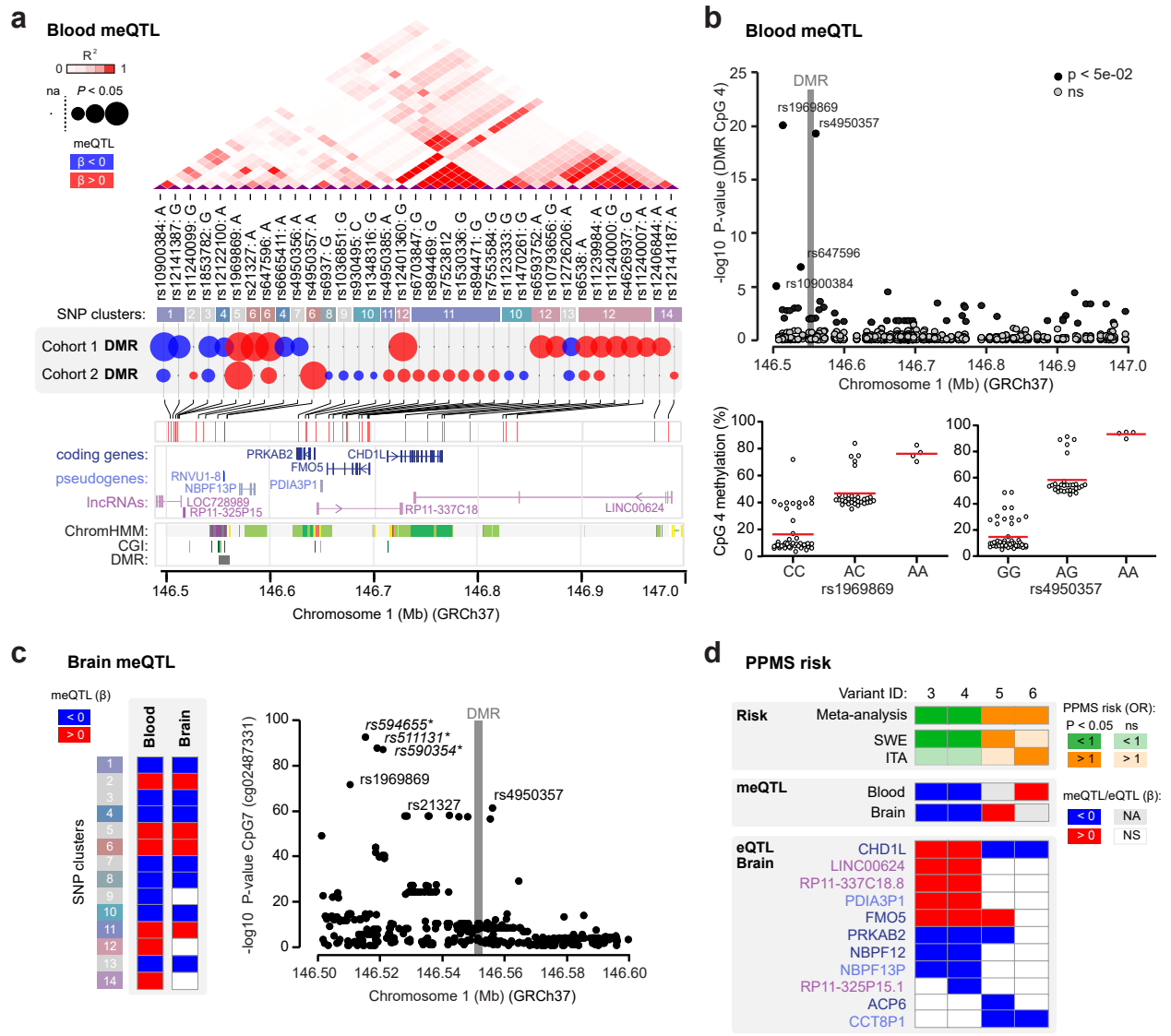
a
Blood meQTL
R²
0
1
na
P < 0.05
meQTL
β < 0
β > 0
rs10900384: A
rs12141387: G
rs11240099: G
rs1853782: G
rs12122100: A
rs1969869: A
rs21327: A
rs647596: A
rs6665411: A
rs4950356: A
rs4950357: A
rs6937: G
rs1036851: G
rs930495: C
rs1348316: G
rs4950385: A
rs12401360: G
rs6703847: G
rs894469: G
rs7523812
rs1530336: G
rs894471: G
rs7555584: G
rs1123333: G
rs1470261: G
rs6593752: A
rs10793656: G
rs12726206: A
rs6538: A
rs1239984: A
rs11240000: G
rs4626937: G
rs11240007: A
rs12406844: A
rs12141187: A
SNP clusters:
1 2 3 4 5 6 6 4 7 6 8 9 10 11 12 11 10 12 13 12 14
Cohort 1 DMR
Cohort 2 DMR
coding genes:
pseudogenes:
lncRNAs:
PRKAB2
CHD1L
FMO5
RNVU1-8
NBPF13P
PDIA3P1
LOC728989
RP11-325P15
RP11-337C18
LINC00624
ChromHMM:
CGI:
DMR:
146.5
146.6
146.7
146.8
146.9
147.0
Chromosome 1 (Mb) (GRCh37)
b
Blood meQTL
DMR
p < 5e-02
ns
rs1969869
rs4950357
rs647596
rs10900384
-log10 P-value (DMR CpG 4)
25
20
15
10
5
0
146.5
146.6
146.7
146.8
146.9
147.0
Chromosome 1 (Mb) (GRCh37)
CpG 4 methylation (%)
100
80
60
40
20
0
CC
AC
AA
rs1969869
GG
AG
AA
rs4950357
c
Brain meQTL
meQTL (β)
< 0
> 0
Blood
Brain
SNP clusters
1
2
3
4
5
6
7
8
9
10
11
12
13
14
rs594655*
rs511131*
rs590354*
rs1969869
rs21327
DMR
rs4950357
-log10 P-value CpG7 (cg02487331)
100
80
60
40
20
0
146.50
146.52
146.54
146.56
146.58
146.60
Chromosome 1 (Mb) (GRCh37)
d
PPMS risk
Variant ID:
3
4
5
6
Risk
Meta-analysis
SWE
ITA
PPMS risk (OR):
P < 0.05
ns
< 1
< 1
> 1
> 1
meQTL
Blood
Brain
meQTL/eQTL (β):
< 0
NA
> 0
NS
eQTL
Brain
CHD1L
LINC00624
RP11-337C18.8
PDIA3P1
FMO5
PRKAB2
NBPF12
NBPF13P
RP11-325P15.1
ACP6
CCT8P1

Figure 4

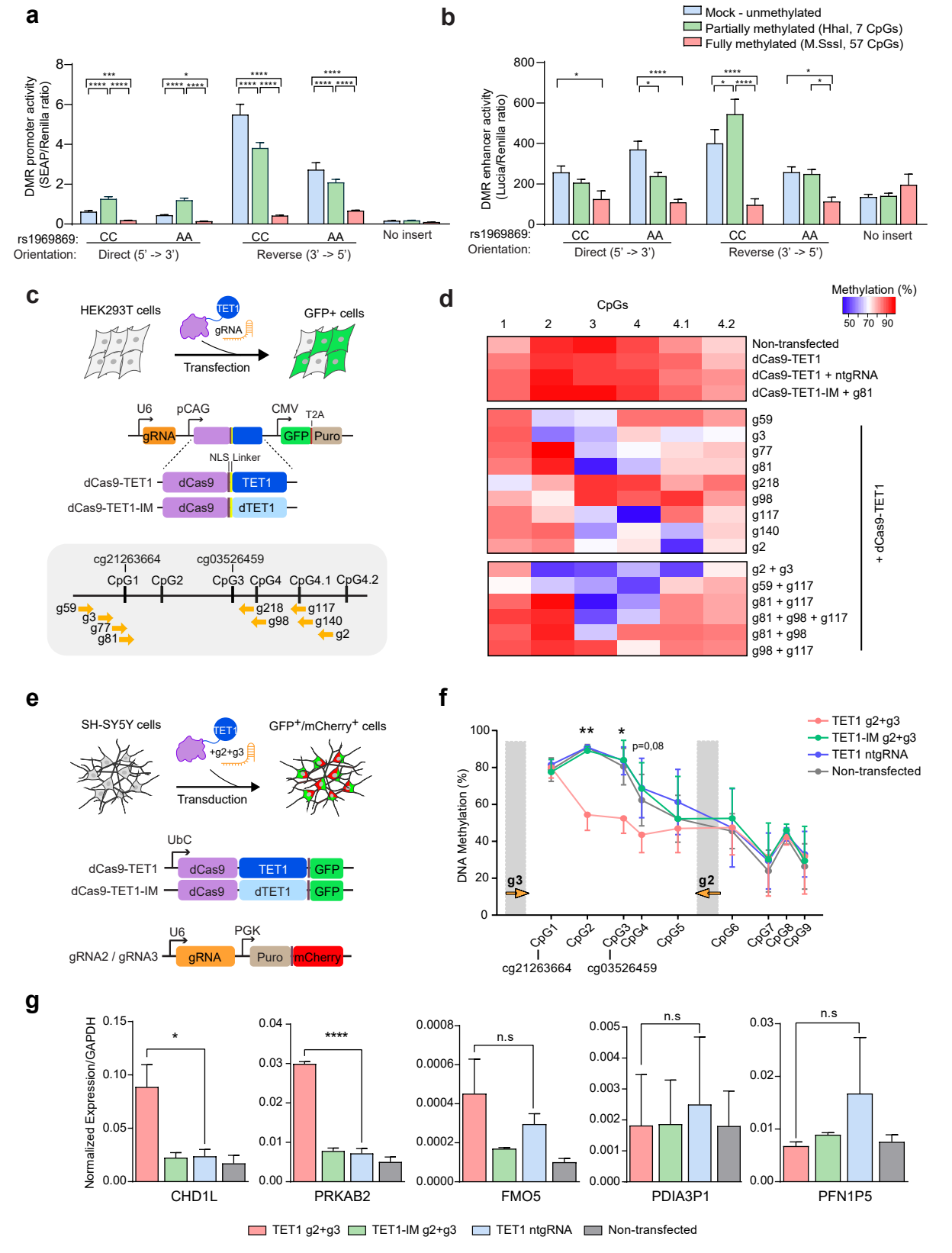
a
DMR promoter activity (SEAP/Renilla ratio)
rs1969869: CC AA CC AA No insert
Orientation: Direct (5' -> 3') Reverse (3' -> 5')
b
Mock - unmethylated
Partially methylated (HhaI, 7 CpGs)
Fully methylated (M.SssI, 57 CpGs)
DMR enhancer activity (Lucia/Renilla ratio)
rs1969869: CC AA CC AA No insert
Orientation: Direct (5' -> 3') Reverse (3' -> 5')
c
HEK293T cells
TET1
gRNA
Transfection
GFP+ cells
U6 pCAG CMV T2A
gRNA GFP Puro
NLS Linker
dCas9-TET1 dCas9 TET1
dCas9-TET1-IM dCas9 dTET1
cg21263664 cg03526459
CpG1 CpG2 CpG3 CpG4 CpG4.1 CpG4.2
g59 g3 g77 g81 g218 g98 g117 g140 g2
d
Methylation (%)
50 70 90
CpGs
1 2 3 4 4.1 4.2
Non-transfected
dCas9-TET1
dCas9-TET1 + ntgRNA
dCas9-TET1-IM + g81
g59
g3
g77
g81
g218
g98
g117
g140
g2
g2 + g3
g59 + g117
g81 + g117
g81 + g98 + g117
g81 + g98
g98 + g117
+ dCas9-TET1
e
SH-SY5Y cells
TET1
+g2+g3
Transduction
GFP+/mCherry+ cells
UbC
dCas9-TET1 dCas9 TET1 GFP
dCas9-TET1-IM dCas9 dTET1 GFP
U6 PGK
gRNA2 / gRNA3 gRNA Puro mCherry
f
TET1 g2+g3
TET1-IM g2+g3
TET1 ntgRNA
Non-transfected
DNA Methylation (%)
p=0,08
g3
g2
CpG1 CpG2 CpG3 CpG4 CpG5 CpG6 CpG7 CpG8 CpG9
cg21263664 cg03526459
g
Normalized Expression/GAPDH
CHD1L
PRKAB2
FMO5
PDIA3P1
PFN1P5
n.s
TET1 g2+g3
TET1-IM g2+g3
TET1 ntgRNA
Non-transfected

Figure 5

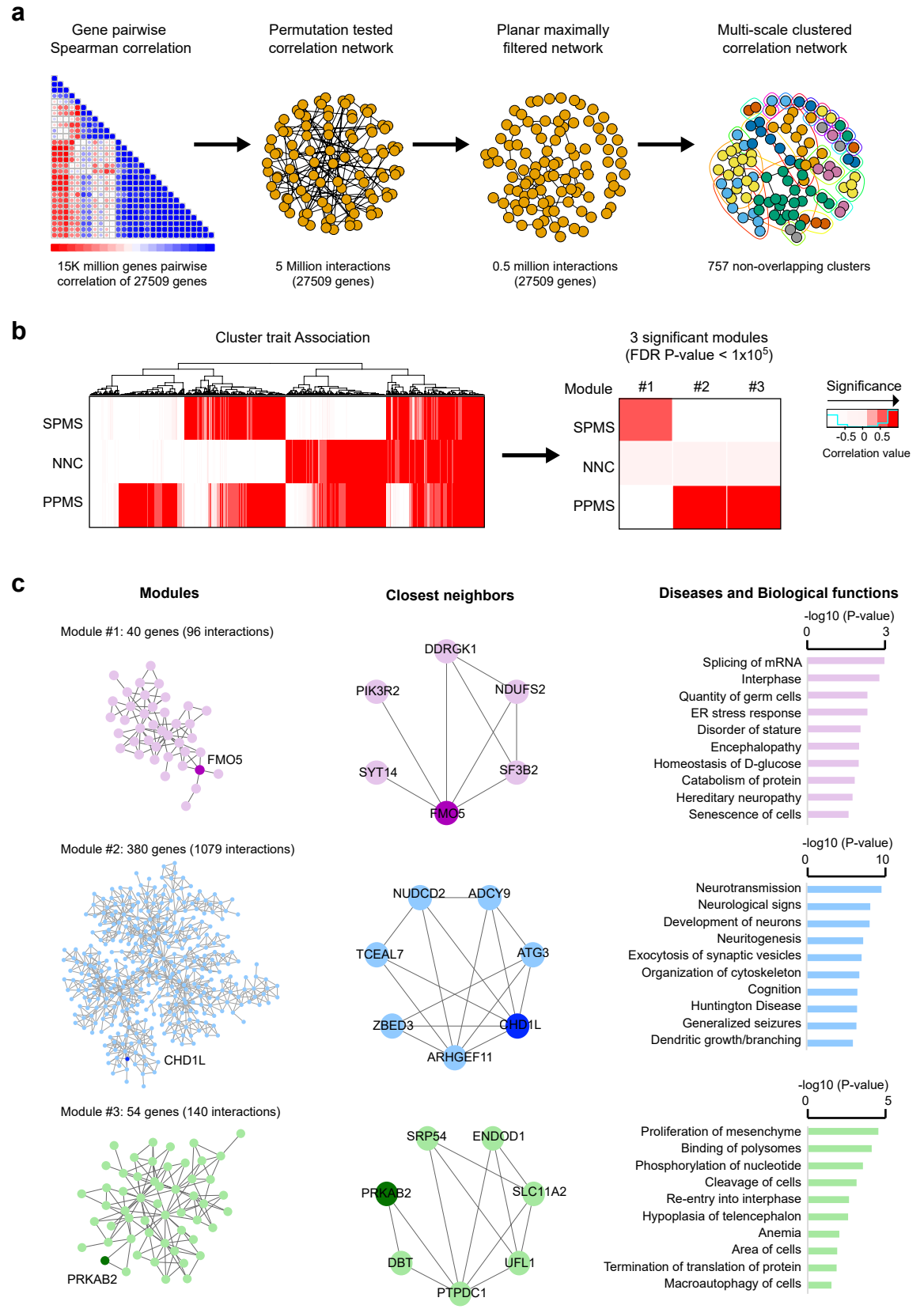
a
Gene pairwise Spearman correlation
Permutation tested correlation network
Planar maximally filtered network
Multi-scale clustered correlation network
15K million genes pairwise correlation of 27509 genes
5 Million interactions (27509 genes)
0.5 million interactions (27509 genes)
757 non-overlapping clusters
b
Cluster trait Association
SPMS
NNC
PPMS
3 significant modules (FDR P-value < 1x10^5)
Module
#1
#2
#3
Significance
-0.5 0 0.5
Correlation value
c
Modules
Closest neighbors
Diseases and Biological functions
Module #1: 40 genes (96 interactions)
FMO5
DDRGK1
PIK3R2
NDUFS2
SYT14
SF3B2
-log10 (P-value)
0
3
Splicing of mRNA
Interphase
Quantity of germ cells
ER stress response
Disorder of stature
Encephalopathy
Homeostasis of D-glucose
Catabolism of protein
Hereditary neuropathy
Senescence of cells
Module #2: 380 genes (1079 interactions)
CHD1L
NUDCD2
ADCY9
TCEAL7
ATG3
ZBED3
ARHGEF11
-log10 (P-value)
0
10
Neurotransmission
Neurological signs
Development of neurons
Neuritogenesis
Exocytosis of synaptic vesicles
Organization of cytoskeleton
Cognition
Huntington Disease
Generalized seizures
Dendritic growth/branching
Module #3: 54 genes (140 interactions)
PRKAB2
SRP54
ENDOD1
SLC11A2
DBT
UFL1
PTPDC1
-log10 (P-value)
0
5
Proliferation of mesenchyme
Binding of polysomes
Phosphorylation of nucleotide
Cleavage of cells
Re-entry into interphase
Hypoplasia of telencephalon
Anemia
Area of cells
Termination of translation of protein
Macroautophagy of cells